Pathological Features of Reinnervated Skeletal Muscles Following Crush Injury of the Sciatic Nerve in Ob/ob Mice

Takahiro Asano
Mie University Graduate School of Medicine Faculty of Medicine: Mie Daigaku Daigakuin Igakukei Kenkyuka Igakubu

Masaya Tsujii (m.tsujii727@gmail.com)
Department of Orthopaedic Surgery, Graduate School of Medicine, Mie University Address: 2-174 Edobashi, Tsu City, Japan https://orcid.org/0000-0002-0167-2824

Takahiro Iino
Mie University Graduate School of Medicine Faculty of Medicine: Mie Daigaku Daigakuin Igakukei Kenkyuka Igakubu

Kazuya Odake
Mie University Graduate School of Medicine Faculty of Medicine: Mie Daigaku Daigakuin Igakukei Kenkyuka Igakubu

Akihiro Sudo
Mie University Graduate School of Medicine Faculty of Medicine: Mie Daigaku Daigakuin Igakukei Kenkyuka Igakubu

Research

Keywords: obesity, skeletal muscle, motor function, ob/ob mice, peripheral nerve disorder

Posted Date: September 15th, 2020

DOI: https://doi.org/10.21203/rs.3.rs-75433/v1

Version of Record: A version of this preprint was published at Muscle & Nerve on July 13th, 2021. See the published version at https://doi.org/10.1002/mus.27365.

Abstract

Background: Obesity is a factor for insufficient improvement of motor function for peripheral nerve disorders. The aims of this study were to evaluate the skeletal muscles during denervation and re-innervation following nerve crush injury in ob/ob mice.

Methods: Experiments were performed on the skeletal muscles of the hindlimbs in 20 male leptin-deficient (ob/ob) mice and control mice. Firstly, the characteristics of the gastrocnemius muscles in the mice were evaluated by histological analysis, immunohistological analysis, and Sircol-collagen assay after measurement of body weight and wet weight of the skeletal muscles and by walking tracking analysis. In the histological analysis, nicotinamide adenine dinucleotide tetrazolium reductase (NADH-TR) staining, oil red O staining, and Picro-sirius red staining were performed to assess the type of myofibers, lipid accumulation, and collagen deposition, respectively. Then, the models for denervation and re-innervation were made by crushing the sciatic nerves with smooth forceps. The same assessments were performed on the skeletal muscles of nerve crush models.

Results: The wet weight of the gastrocnemius muscles was significantly less in the ob/ob mice than the control mice, whereas body weight was significantly more. Histological analyses demonstrated a smaller cross-sectional area of type II fibers and increase of type I fiber grouping of the skeletal muscles in the ob/ob mice. In addition, there was excessive deposition of lipids and collagens between the myofibers. Following the nerve injury, the recovery of motor function was equal between both groups, while the cross-sectional area of type II fibers was significantly smaller in the ob/ob mice than the control mice at 4 weeks. Furthermore, the denervated muscles showed an increase in collagen deposition to the area of intermyofibers, which were predominant in the ob/ob mice after the nerve injury.

Conclusions: The present study showed an increase of collagen deposition, delayed recovery of type II myofibers, and type I fiber grouping during denervation and re-innervation in the skeletal muscles of ob/ob mice. We suggest through these findings that the reduction of contractile force could be one of causes of insufficient improvement in peripheral nerve disorders of obese individuals.

Background

The recovery of motor strength and sensory deficiency are the goals of treatment for peripheral nerve disorders including entrapment neuropathies and spinal disorders. Nonetheless, clinicians have occasionally encountered patients with insufficient improvement of motor function, whereas denervated muscles due to disorders of the peripheral nerves could be recovered by proper treatment facilitating axonal regeneration, which results in re-innervation to the skeletal muscles. The insufficiency is a serious problem because the reduction of muscle strength has a potentially devastating outcome on daily activity.

For functional recovery after peripheral nerve injury, the condition of the distal portion, including denervated muscle and the distal stump of the injured nerve, is likely to be more crucial than the proximal

portion [1]. Most researchers have paid attention to the pathophysiology of the peripheral nervous system for recovery of peripheral nerve injuries [2, 3], whereas we can find few studies regarding the pathophysiology of skeletal muscles in processes during denervation and re-innervation. The denervation-induced skeletal muscles have biochemical and physiological changes including loss of muscle mass, reduction in the number of satellite cells, and formation of fibrotic tissue [4, 5]. In addition, underlying disease may aggravate the denervation and re-innervation process of the skeletal muscles.

Obesity, one of the metabolic syndromes, is characterized by elevated adipose storage in subcutaneous and visceral tissues and non-adipose organs, a phenomenon called ectopic lipid accumulation [6, 7]. Owing to deposition of lipids, inflammation and fibrosis are caused to various organs including the heart and liver, leading to diastolic dysfunction and non-alcoholic steatohepatitis (NASH), respectively [8, 9]. These conditions finally progress to serious disorders including heart failure and liver cirrhosis. The skeletal muscles are also a target organ of ectopic lipid accumulation in obese individuals, by which inflammation and fibrosis impair skeletal muscle function [10]. Taken together, we suspect there could exist excessive deposition of collagen due to both denervation and lipid toxicity in the denervated muscles of obese individuals with peripheral nerve disorders.

Leptin-deficient (ob/ob) mice become insulin resistant due to deficiency of leptin and develop severe obesity. These animals have been used for various studies in the pathophysiology of the diseases related to obesity including cardiovascular disease, renal disorders, and diabetic mellitus. Previous studies show that the number of non-myelinated fibers decreased in ob/ob mice compared with control mice, whereas there existed no change of the number of myelinated nerve fibers, such as motor nerve fibers [3]. Nonetheless, we could find no research regarding the skeletal muscles during re-innervation in the animal model of obesity following denervation due to peripheral nerve injuries.

Besides, shifts in fiber type could also be the cause of insufficiency of skeletal muscle function during re-innervation. A previous study demonstrated that the process of re-innervation was faster in type I fibers than type II fibers [11]. As a result, re-innervation to type I fibers led to an increase of fiber type grouping of type I fibers in reinnervated muscles. In addition, several investigators showed an increase of type I fibers and a decrease of type II fibers with advanced age [11]. Therefore, it should be understood whether there would be differences of fiber type in reinnervated muscles under chronic inflammation conditions such as obesity.

The purposes of this study are 1) to evaluate the skeletal muscle in ob/ob mice, 2) to assess the myofibers and the deposition of lipids and collagen on skeletal muscles after denervation in ob/ob mice, 3) to evaluate the fiber type of reinnervated skeletal muscles.

Methods

Subjects

Experiments were performed on 20 male C57/BL6-ob/ob mice and the same number of their control strain, C57/BL6 mice (10 weeks old; SLC, Hamamatsu, Japan). The animals were housed in a temperature-controlled environment and maintained on a 12-hour light-dark cycle with food and water available *ad libitum*. The experimental protocol was approved by the committee of animal research at Mie University.

Surgical Procedure

The mice were deeply anesthetized with an intraperitoneal injection of sodium pentobarbital (0.05 mg/g body weight) following the measurement of body weight. For sciatic nerve crush, a longitudinal cutaneous incision was made on the right hind limb under aseptic conditions. Then, the sciatic nerve was exposed by separation of the gluteal muscle, and crushed with smooth forceps for 15 seconds at the level of the sciatic notch, according to previously reported methods [12, 13]. The indentation of the sciatic nerve was confirmed; the skin incision was closed with 5 − 0 surgical suture. At 1, 2, and 4 weeks after the surgery (n = 5 at each week), the skeletal muscles of gastrocnemius and tibialis anterior were fully excised from the attachment site. After the measurement of the muscles' wet weight, the gastrocnemius muscles were immersed in isopentane and cooled to freezing point with liquid nitrogen for 10–20 sec, to allow complete freezing to make frozen muscle tissue specimens [14]. The tibialis anterior muscles were snap frozen with liquid nitrogen for the collagen assays. In addition, the other five mice in each ob/ob and control group served as normal controls, and the skeletal muscles were collected.

Footprint Recording And Sciatic Functional Index (sfi) Analysis

A walking track analysis was performed based on previous methods [15–17], before and at 1, 2, and 4 weeks after the nerve crush. The total spread (TS), print length (PL), and intermediate toes were measured on the experimental (nerve crushed) side (E) and the contralateral normal side (N), in each mouse. Ten footprints per mouse and a total of 250 footprints were measured. The sciatic functional index (SFI) of each animal was calculated by the following formula: SFI = -38.3((EPL - NPL)/NPL) + 109.5((ETS - NTS)/NTS) + 13.3((EITS - NITS)/NITS) − 8.8. In general, SFI oscillates around 0 for normal nerve function; whereas around − 100 SFI represents total dysfunction.

Histological Analysis

The frozen specimens of the gastrocnemius muscle were transversely cut to 10 μm at the center of the muscle using a cryostat. The tissue sections were subjected to nicotinamide adenine dinucleotide tetrazolium reductase (NADH-TR) staining, oil red O staining, and Picro-sirius red staining according to standard protocols, for muscle fiber type indication, lipid droplets, and collagen deposition, respectively. The images of the stained sections were obtained at a magnification of 200x using an optical

microscope (BX50; Olympus, Tokyo, Japan). On the NADH stained sections in 15 random fields, the number of each myofiber type was counted using image analysis software (Lumina Vison, MITANI, Japan). In addition, the improvement rates were calculated based on the number of myofibers in the normal control. The percentage of enclosed type I fibers was also determined to evaluate the degree of fiber type grouping. The grouping was considered enclosed if a type I fiber was completely surrounded by type II fibers within the same muscle bundle. Moreover, areas of lipids droplets and collagen deposition between myofibers were measured using the same software. The areas were compared between the sections of the normal controls and the ob/ob mice at 4 weeks after nerve crush.

Immunohistochemistry

Immunohistochemical analysis was performed with a rabbit polyclonal anti-Perilipin-1 antibody (Cell Signaling Technology, MA, USA) for proliferation of adipocytes. On the frozen specimens of the gastrocnemius muscle, endogenous peroxidase was inactivated by 0.3% hydrogen peroxide in methanol for 30 minutes. The sections were incubated with the primary antibody overnight at 4 °C. Between the incubation steps, sections were dip-immersion washed (3 · 5-minute wash) in tris-buffered saline (TBS) to eliminate excesses of non-bound antibodies or reagent. The antibody was diluted in 1% BSA/TBS to suppress nonspecific reactions. Then, the sections were incubated with the anti-rabbit immunoglobulin conjugate horseradish peroxidase (HRP) and anti-mouse immunoglobulin conjugate HRP mixed in by employing the universal immuno-enzyme polymer method (Histofine® Simple Stain MAX-PO; Nichirei, Tokyo, Japan). The reaction products were visualized in 0.15 mg/ml 3,3’-diaminobenzidine tetrahydrochloride (DAB) solution containing 0.003% hydrogen peroxide. After washing in water, the counter was stained by hematoxylin.

Sircol-collagen Assay (sca)

The muscles of the tibialis anterior muscle frozen with liquid nitrogen were excised into 40 mg pieces and homogenized; immersed in 400 µl of 0.5 M acetic acid with stirring for 12 hours, centrifuged at 15,000 g x 60 min, and the supernatants were collected. The extracted collagen was measured according to SCA protocol (Sircol soluble collagen assay kit, Biocolor, China). Spectrophotometric readings were taken at 540 nm on a Fluostar Optima microplate reader. Absolute values were attained with a standard graph composed from collagen type I standard supplied with the kit in the range 5–50 µg per 100 µl. The values were expressed as percentage by muscle wet weight.

Statistical analysis

Analyses were performed with SPSS version 22.0 statistical package (SPSS Inc., Chicago, IL, USA). Data between ob/ob and control mice were analyzed using the Mann–Whitney *U* test. $P < 0.05$ was considered statistically significant.

Results

Skeletal muscles in ob/ob mice had small cross-sectional area of type II fibers with excessive deposition of lipid and collagen in the area of the intermyofibers

Body weights of ob/ob mice were 41.9 ± 2.3 g (mean ± SD) at 10 weeks after the birth, and were significantly heavier than that of control mice 25.4 ± 1.2 g ($p < 0.01$). In contrast, muscle wet weights of both tibialis anterior and gastrocnemius of ob/ob mice were lower in ob/ob mice (35.3 ± 2.1 mg and 97.5 ± 9.3 mg, respectively) than control mice (47.9 ± 2.7 mg and 127.9 ± 7.9 mg, respectively) ($p < 0.01$) (Fig. 1). Histological analysis demonstrated that the size of the cross-sectional area in type II fiber was significantly smaller in ob/ob mice (1459.0 ± 392.2 μm^2) than that in control mice (2355.0 ± 610.0 μm^2) ($p < 0.05$). The percentage of enclosed type I fibers was also significantly higher in ob/ob mice (1.4 ± 1.7%) than that in control mice (7.0 ± 5.1%) ($p < 0.01$). Meanwhile, the sizes of type I fibers were not different between both groups (Fig. 2). Furthermore, the area of lipid droplets and collagen deposition and the number of adipocytes were significantly larger in ob/ob mice compared with controls (Fig. 3, 4) ($p < 0.05$). Skeletal muscle collagen levels measured by SCA also showed significantly higher collagen content in skeletal muscle in ob/ob mice (4.7 ± 0.3%) than in the control group (3.0 ± 0.4%; $p < 0.05$).

Recovery of motor function was equal between ob/ob and control mice following the nerve injury, even though the cross-sectional area of type II fibers was small in ob/ob mice

SFI was immediately reduced after crush and then gradually improved until 4 weeks (-108.1 ± 17.0 at 1 day, -26.1 ± 5.4 at 4 weeks after crush). The ob/ob mice showed a slight tendency for low SFI at 1 day, and at 4 weeks (-115.7 ± 11.3, -27.0 ± 16.2, respectively), but no significant difference was observed between the two groups, and the ob/ob mice showed equal improvement at 4 weeks (Fig. 5). Furthermore, cross-sectional areas in both type I and type II fibers of the gastrocnemius muscles were predominantly decreased in ob/ob mice as well as control mice at 1 week after nerve crush. Thereafter, the cross-sectional areas were increased in type I and type II fibers at 1 week and 2 weeks later after the nerve injury. In control mice, the cross-sectional areas were recovered up to 86.2 ± 1.4% and 83.1 ± 9.2% of the non-affected side in type I and type II fibers at 4 weeks after the nerve injury, respectively. By contrast, the ob/ob mice had an improvement of 79.6 ± 8.9% of cross-sectional area in type I fibers, but had insufficient improvement of 71.2 ± 6.9% of the non-affected side in type II fibers. In addition, there was a significant difference of the cross-sectional areas of type II fibers after the nerve injury ($p < 0.05$) (Fig. 6). Moreover, the percentage of enclosed type I fibers was increased in both the ob/ob and control groups (13.7 ± 2.3% and 4.2 ± 4.0%, respectively). It significantly increased in ob/ob mice ($p < 0.05$) (Fig. 7).

Collagen deposition was increased due to nerve injury, especially in ob/ob mice

Furthermore, we noticed the increase of collagen deposition after the nerve injury on specimens for histological analysis. Picro-sirius red staining showed that collagen deposition was clearly increased between fibers in the skeletal muscles at 4 weeks after the nerve injuries in both ob/ob and control mice. Especially, the increase of the collagen was predominant in ob/ob mice, and the rates of collagen area

were significantly larger in specimens of ob/ob mice than in the control mice ($p < 0.05$), regardless of the crush injury to the nerves (Fig. 8). SCA also showed that the amount of collagen was 8.3 ± 2.4% in the reinnervated muscles of ob/ob mice following the crush injury of the sciatic nerve, which was significantly higher compared to ob/ob and control mice without the nerve injury (4.7 ± 0.3% and 3.0 ± 0.4%, respectively) ($p < 0.05$) (Fig. 9).

Discussion

The skeletal muscles in ob/ob mice had a smaller cross-sectional area in type II fibers, with excessive deposition of lipid and collagen in the area of the intermyofibers, when compared to the control group. Despite this, the recovery of motor function was equal between ob/ob and control mice following the nerve injury. Collagen deposition was increased both groups due to nerve injury, especially in ob/ob mice.

Obesity is a causative factor for the disorders of various organs including cardiovascular tissues and the liver, which is a target of ectopic lipid accumulation. The excessive lipid accumulation to the non-adipose tissues can cause cell dysfunction or cell death via pro-inflammation, and these processes have been defined as lipotoxicity [18]. As a result, inflammation and fibrosis are caused to the heart and the liver, leading to diastolic dysfunction of the heart and non-alcoholic steatohepatitis (NASH), respectively [8, 9]. Consequently, these conditions can progress to serious conditions including heart failure and liver cirrhosis. The lipotoxicity is a concern for the skeletal muscles, since skeletal muscles are also a target for ectopic lipid accumulation in individuals with obesity. In fact, we found a number of studies regarding the pathophysiology of the lipotoxicity to skeletal muscle cells based on *in vitro* study [19, 20], while the adverse effect of lipotoxicity *in vivo* and the functional consequences are unresolved.

In the present study, we used ob/ob mice as the animal model of obesity, in which lipid accumulation and increases of adipocytes were clearly shown in the gastrocnemius muscles. Therefore, the ob/ob mice are an appropriate model of *in vivo* exploration into the adverse effect of lipotoxicity to the skeletal muscles. Furthermore, the skeletal muscles were observed to be atrophic in the ob/ob mice, in which reduction of cross-sectional areas of type II fibers was predominant. In addition, the skeletal muscles had more collagen deposition between the myofibers in the ob/ob mice than in the control mice. These findings are similar to those in liver and heart patients with obesity [21, 22], suggesting that the skeletal muscles in the obese subjects could be atrophic through chronic inflammation owing to lipotoxicity. In fact, a previous study showed that obese adults had a reduction of quadriceps muscle strength relative to body mass compared to non-obese adults [23].

Furthermore, previous studies reported that patients with obesity had inferior function in comparison to non-obese patients after surgery for peripheral nerve disorders, even though the surgical treatments had good clinical results in comparison to the preoperative condition. Roh et al. stated that patients with metabolic syndrome, which is strongly related to obesity, had decreased pinch strength and delay of functional recovery after the surgical treatment for carpal tunnel syndrome [24]. Burgstaller et al. described fewer obese patients with meaningful improvement than non-obese individuals in the surgical

treatment for lumbar canal stenosis [25]. These studies suggest obesity is associated with insufficient improvement due to impairment during the denervation and re-innervation process in the surgical treatment of peripheral disorders.

Nonetheless, the improvements in the functional status were equal between ob/ob and control mice after the nerve injury, while histological analysis showed that recovery of the cross-sectional area in type II fibers was delayed and poor in the ob/ob mice than in the control mice. In general, type I fibers are associated with endurance, while type II fibers are characterized as 'fast fibers', and associated with strength of skeletal muscles [26]. The results might indicate inferior recovery of muscle strength after the nerve injury in patients with obesity, even though the muscle strength was not measured in this study. By contrast, the recovery of cross-sectional area of type I fibers was not different between the two groups, which is likely to explain the reason for no difference in functional status.

Likewise, an increase of type I fiber grouping was observed in the ob/ob mice, especially after the nerve injury. Previous studies have demonstrated that re-innervation of type I fibers is faster than that of type II fibers, in which preferential re-innervation of type I fibers in recovery following nerve injury leads to an increase in type I grouping in reinnervated muscles [11, 27]. Furthermore, shifts of fiber groupings are associated with aging in the denervation and re-innervation processes, suggesting that an increase of type I grouping might influence the function of reinnervated muscles, such as contraction of the myofibers [11]. This study suggests obesity could not only cause a shift of fiber type in the skeletal muscles which result in decreased muscular strength, but also cause insufficient recovery after the nerve injury.

Furthermore, the collagen deposition on the intermyofibers was increased in the skeletal muscles following the nerve injury [28]. The fibrotic formation is characterized by an anomalous accumulation of the extracellular matrix, such as collagen around inflamed tissues, and leads to the dysfunction in various tissues including the heart and liver [29]. In myocardial tissue, this reactive and progressive interstitial fibrosis contributes to myocardial stiffness with progression to ventricular dysfunction. Even though the pathological significance of the fibrosis is less elucidated in the skeletal muscles than in other organs, fibrosis of the skeletal muscle is a characteristic feature of muscular dystrophin, myopathies, and traumatic injuries [30]. In addition, previous studies show that fibrosis caused a decrease in skeletal muscular strength [31–33]. Therefore, abnormal accumulation of fibrotic tissues, which were observed in the denervated and reinnervated muscles of ob/ob mice, also may lead to stiffness of the skeletal muscles and result in a reduction of contractile force. In the future, reduction of body weight, anti-fibrotic drugs, and inhibition of fatty acid for the recovery of motor function in peripheral nerve disorders need to be evaluated.

In conclusion, this study showed that the skeletal muscles of ob/ob mice were smaller in cross-sectional area of type II fibers with excessive deposition of lipid and collagen at the interstitial area at myofibers. Following injury of the sciatic nerve, recovery of motor function was equal between ob/ob and control mice following nerve injury, whereas the skeletal muscles of ob/ob mice not only had a significantly

smaller sectional area of type II fibers than the control mice, but also comprised an increase of type I fiber grouping during denervation and re-innervation. In addition, collagen deposition was significantly increased in the skeletal muscles of the ob/ob mice after the nerve injury. We suggest that lipotoxicity to type II fibers, grouping of type I fibers, and interstitial fibrosis due to collagen deposition could be the causes of insufficient improvement after surgery for peripheral nerve injury in obese individuals.

List Of Abbreviations

PL	Print length
SCA	Sircol-collagen assay
SFI	Sciatic functional index
TBS	Tris-buffered saline
TS	Total spread

Declarations

Ethics approval and consent to participate

All procedures involving animals were approved by the committee of animal research at Mie University.

Consent for publication

Not applicable.

Availability of data and material

The datasets used and/or analyzed during the current study are available from the corresponding author on reasonable request.

Competing interests

The authors declare that they have no competing interests.

Funding

Not applicable.

Authors' contributions

TA and MT designed the research and wrote the paper. TI participated in the experimental design and techniques. All authors read and approved the final manuscript.

Acknowledgements

We thank Katsura Chiba for help the experimental techniques. This study was supported by Department of Orthopaedic Surgery, Graduate School of Medicine Mie University and the committee of animal research at Mie University.

References

1. Gordon T, Tyreman N, Raji MA. The basis for diminished functional recovery after delayed peripheral nerve repair. J Neurosci. 2011;31:5325–34.
2. Bekar E, Altunkaynak BZ, Balcı K, Aslan G, Ayyıldız M, Kaplan S. Effects of high fat diet induced obesity on peripheral nerve regeneration and levels of GAP 43 and TGF-beta in rats. Biotech Histochem. 2014;89:446–56.
3. Nowicki M, Kosacka J, Serke H, Blüher M, Spanel-Borowski K. Altered sciatic nerve fiber morphology and endoneural microvessels in mouse models relevant for obesity, peripheral diabetic polyneuropathy, and the metabolic syndrome. J Neurosci Res. 2012;90:122–31.
4. Gwag T, Park K, Park J, Lee JH, Nikawa T, Choi I. Celastrol overcomes HSP72 gene silencing-mediated muscle atrophy and induces myofiber preservation. J Physiol Pharmacol. 2015;66:273–83.
5. Soldado F, Fontecha CG, Marotta M, Benito D, Casaccia M, Mascarenhas VV, et al. The role of muscle imbalance in the pathogenesis of shoulder contracture after neonatal brachial plexus palsy: a study in a rat model. J Shoulder Elbow Surg. 2014;23:1003–9.
6. Kim B, Feldman EL. Insulin resistance in the nervous system. Trends Endocrinol Metab. 2012;23:133–41.
7. Yaffe K, Kanaya A, Lindquist K, Simonsick EM, Harris T, Shorr RI, et al. The metabolic syndrome, inflammation, and risk of cognitive decline. J Am Med Assoc. 2004;292:2237–42.
8. Aroor AR, Habibi J, Kandikattu HK, Garro-Kacher M, Barron B, Chen D, et al. Dipeptidyl peptidase-4 (DPP-4) inhibition with linagliptin reduces western diet-induced myocardial TRAF3IP2 expression, inflammation and fibrosis in female mice. Cardiovasc Diabetol. 2017;16:61.
9. Kohli R, Kirby M, Xanthakos SA, Softic S, Feldstein AE, Saxena V, et al. High-fructose, medium chain trans fat diet induces liver fibrosis and elevates plasma coenzyme Q9 in a novel murine model of obesity and nonalcoholic steatohepatitis. Hepatology. 2010;52:934–44.
10. Akhmedov D, Berdeaux R. The effects of obesity on skeletal muscle regeneration. Front Physiol. 2013;4:371.
11. Larkin LM, Kuzon WM Jr, Halter JB. Effects of age and nerve-repair grafts on reinnervation and fiber type distribution of rat medial gastrocnemius muscles. Mech Ageing Dev. 2003;124:653–61.
12. Ma CH, Omura T, Cobos EJ, Latrémolière A, Ghasemlou N, Brenner GJ, et al. Accelerating axonal growth promotes motor recovery after peripheral nerve injury in mice. J Clin Invest. 2011;121:4332–47.

13. Morrison BM, Tsingalia A, Vidensky S, Lee Y, Jin L, Farah MH, et al. Deficiency in monocarboxylate transporter 1 (MCT1) in mice delays regeneration of peripheral nerves following sciatic nerve crush. Exp Neurol. 2015;263:325–38.
14. Meng H, Janssen PM, Grange RW, Yang L, Beggs AH, Swanson LC, et al. Tissue triage and freezing for models of skeletal muscle disease. JoVE. 2014;89:e51586.
15. Bain JR, Mackinnon SE, Hunter DA. Functional evaluation of complete sciatic, peroneal, and posterior tibial nerve lesions in the rat. Plast Reconstr Surg. 1989;83:129–38.
16. Wang T, Ito A, Aoyama T, Nakahara R, Nakahata A, Ji X, et al. Functional evaluation outcomes correlate with histomorphometric changes in the rat sciatic nerve crush injury model: A comparison between sciatic functional index and kinematic analysis. PLoS One. 2018;13:e0208985.
17. Kokubu N, Tsujii M, Akeda K, Iino T, Sudo A. BMP-7/Smad expression in dedifferentiated Schwann cells during axonal regeneration and upregulation of endogenous BMP-7 following administration of PTH (1–34). J Orthop Surg. 2018;26:2309499018812953.
18. Unger RH. Minireview: weapons of lean body mass destruction: the role of ectopic lipids in the metabolic syndrome. Endocrinology. 2003;144:5159–65.
19. Hassan RH, Hainault I, Vilquin JT, Samama C, Lasnier F, Ferre P, et al. Endoplasmic reticulum stress does not mediate palmitate-induced insulin resistance in mouse and human muscle cells. Diabetologia. 2012;55:204–14.
20. Irrcher I, Ljubicic V, Hood DA. Interactions between ROS and AMP kinase activity in the regulation of PGC-1alpha transcription in skeletal muscle cells. Am J Physiol Cell Physiol. 2009;296:C116-23.
21. Zhang M, Xie ZF, Zhang RT, Chen DK, Gu M, Cui SC, et al. Novel substituted pyrazolone derivatives as AMP-activated protein kinase activators to inhibit lipid synthesis and reduce lipid accumulation in ob/ob mice. Acta Pharmacol Sin. 2018;39:1622–32.
22. Torre-Villalvazo I, Gonzalez F, Aguilar-Salinas CA, Tovar AR, Torres N. Dietary soy protein reduces cardiac lipid accumulation and the ceramide concentration in high-fat diet-fed rats and ob/ob mice. J Nutr. 2009;139:2237–43.
23. Maffiuletti NA, Jubeau M, Munzinger U, Bizzini M, Agosti F, De Col A, et al. Differences in quadriceps muscle strength and fatigue between lean and obese subjects. Eur J Appl Physiol. 2007;101:51–9.
24. Roh YH, Lee BK, Noh JH, Oh JH, Gong HS, Baek GH. Effects of metabolic syndrome on the outcome of carpal tunnel release: a matched case-control study. J Hand Surg Am. 2015;40:1303–9.
25. Burgstaller JM, Held U, Brunner F, Porchet F, Farshad M, Steurer J, et al. The impact of obesity on the outcome of decompression surgery in degenerative lumbar spinal canal stenosis: analysis of the lumbar spinal outcome study (LSOS): a Swiss prospective multicenter cohort study. Spine. 2016;41:82–9.
26. Lee S, Kim C, Kwon D, Kim MB, Hwang JK. Standardized Kaempferia parviflora Wall. ex Baker (Zingiberaceae) extract inhibits fat accumulation and muscle atrophy in ob/ob mice. Evid Based Complement Alternat Med. 2018;2018:8161042.

27. Yoshimura K, Asato H, Cederna PS, Urbanchek MG, Kuzon WM Jr. The effect of reinnervation on force production and power output in skeletal muscle. J Surg Res. 1999;81:201–8.
28. Liu F, Tang W, Chen D, Li M, Gao Y, Zheng H, et al. Expression of TGF-β1 and CTGF is associated with fibrosis of denervated sternocleidomastoid muscles in mice. Tohoku J Exp Med. 2016;238:49–56.
29. Wynn TA. Cellular and molecular mechanisms of fibrosis. J Pathol. 2008;214:199–210.
30. Mahdy MAA. Skeletal muscle fibrosis: an overview. Cell Tissue Res. 2019;375:575–88.
31. Acuña MJ, Pessina P, Olguin H, Cabrera D, Vio CP, Bader M, et al. Restoration of muscle strength in dystrophic muscle by angiotensin-1-7 through inhibition of TGF-β signalling. Hum Mol Genet. 2014;23:1237–49.
32. Kumar A, Bhatnagar S, Kumar A. Matrix metalloproteinase inhibitor batimastat alleviates pathology and improves skeletal muscle function in dystrophin-deficient mdx mice. Am J Pathol. 2010;177:248–60.
33. Morales MG, Gutierrez J, Cabello-Verrugio C, Cabrera D, Lipson KE, Goldschmeding R, et al. Reducing CTGF/CCN2 slows down mdx muscle dystrophy and improves cell therapy. Hum Mol Genet. 2013;22:1237–49.

Figures

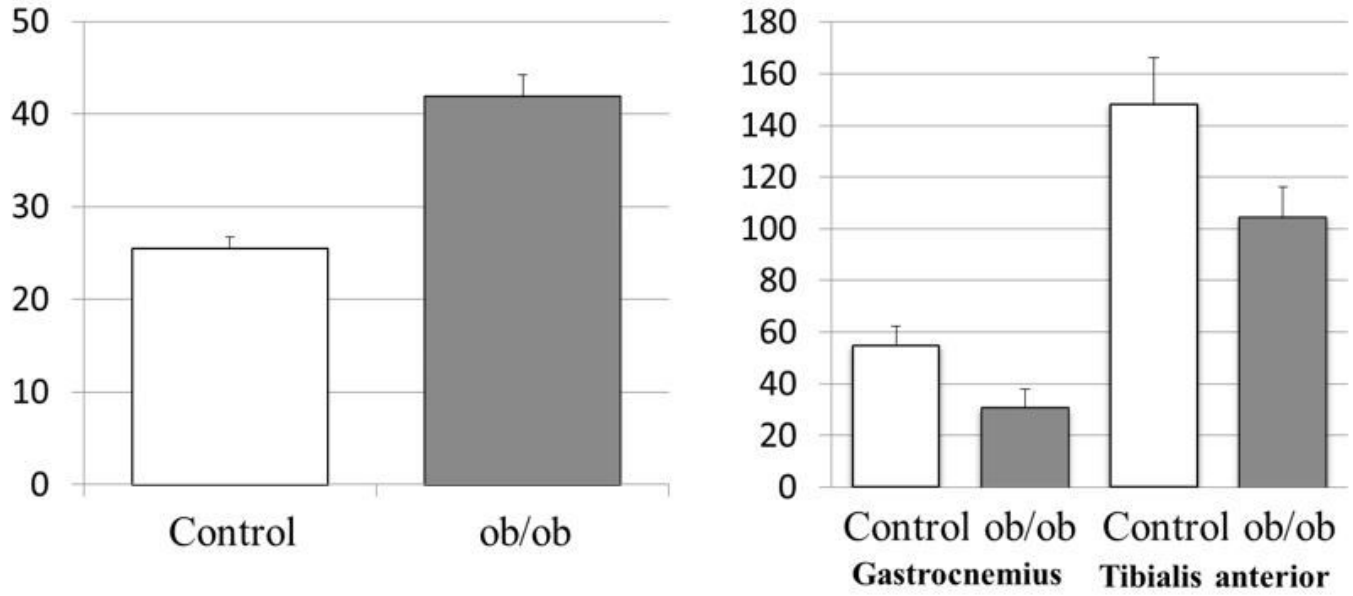

Figure 1

Body weight and muscle wet weight The muscle wet weight of ob/ob mice is significantly less than that of the control mice in both the tibialis anterior and gastrocnemius muscles. *Mann–Whitney U test

p<0.01.

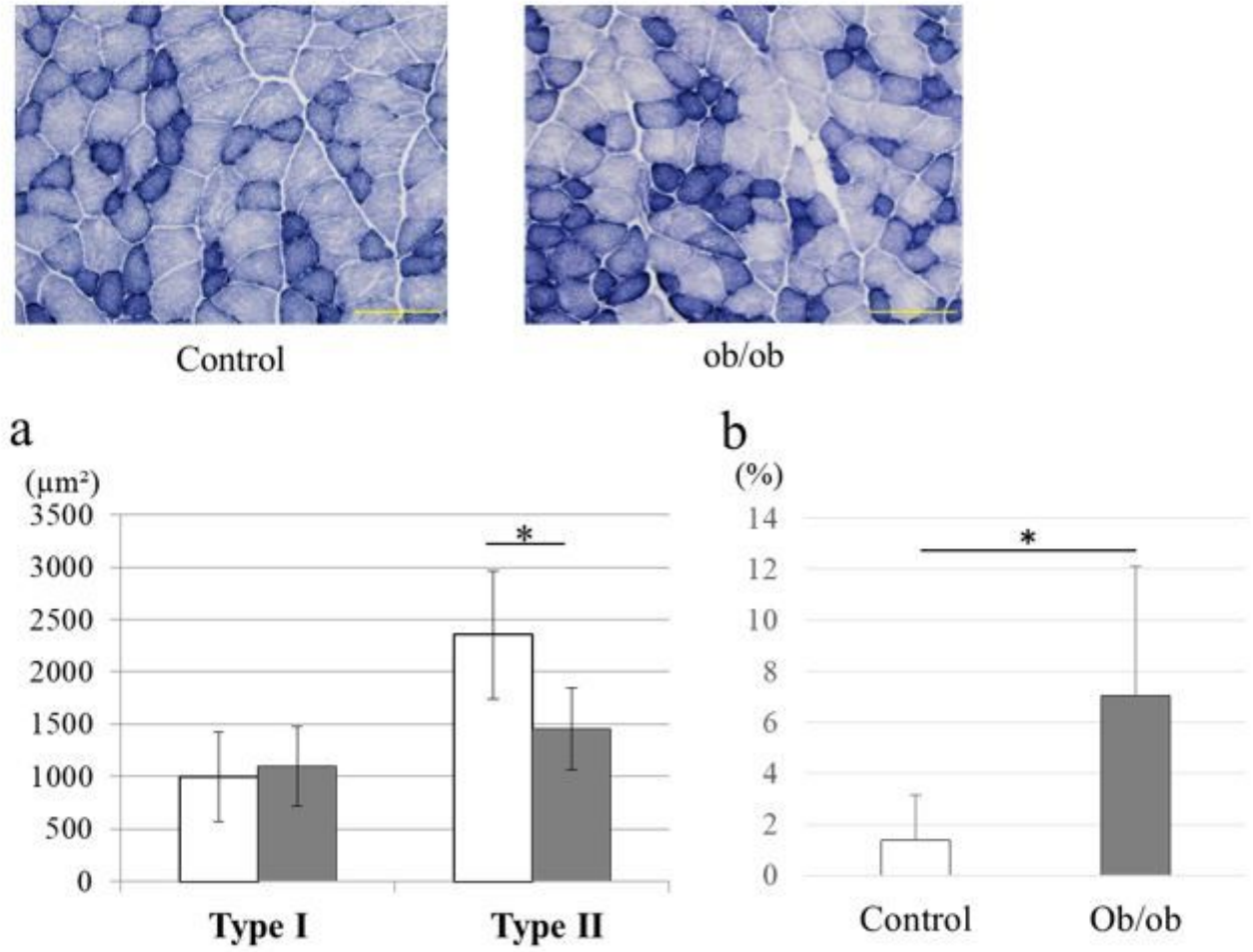

Figure 2

NADH staining a: The size of the type II fiber cross-sectional area is significantly smaller in ob/ob mice than in the control mice. b: The percentage of enclosed type I fibers in ob/ob mice is significantly higher. *p<0.05.

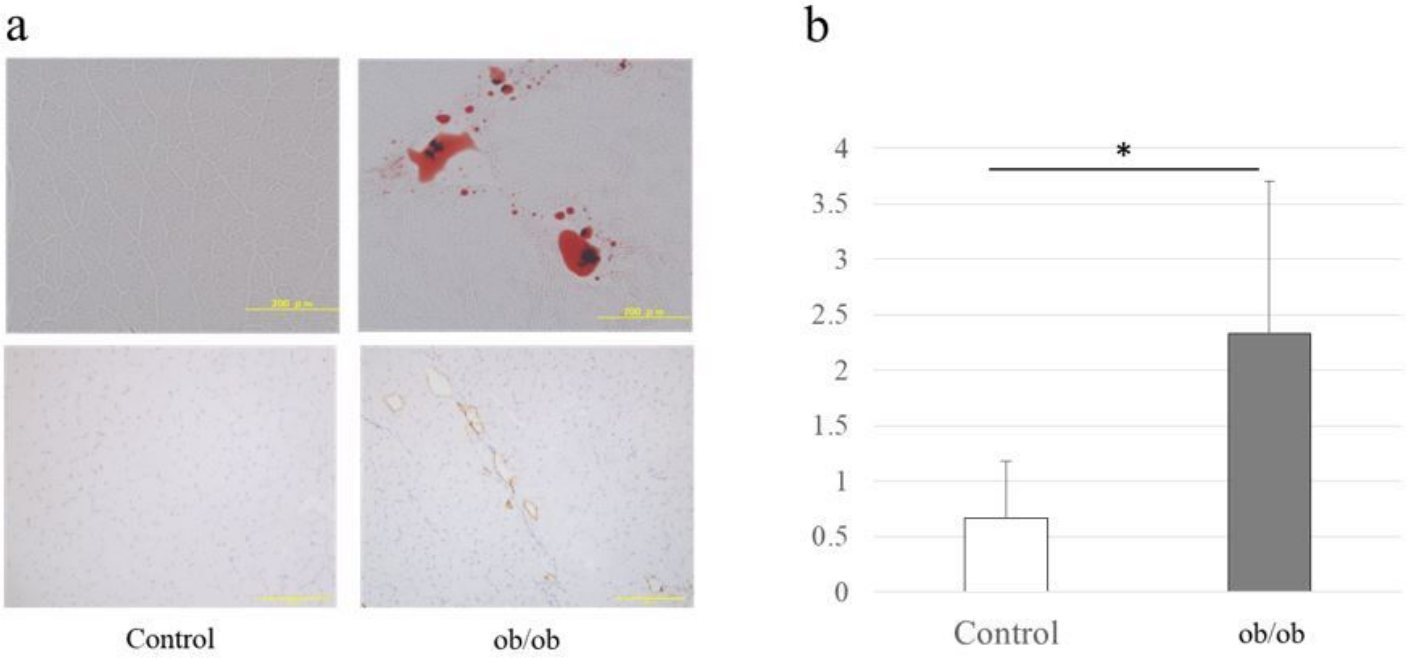

Figure 3

Lipid droplets and adipocytes in skeletal muscle a: Lipid droplets in Oil red O staining and adipocytes in perilipin immunostaining are more visible in ob/ob mice. b: The number of adipocytes in skeletal muscle of ob/ob mice is significantly higher. *p<0.05.

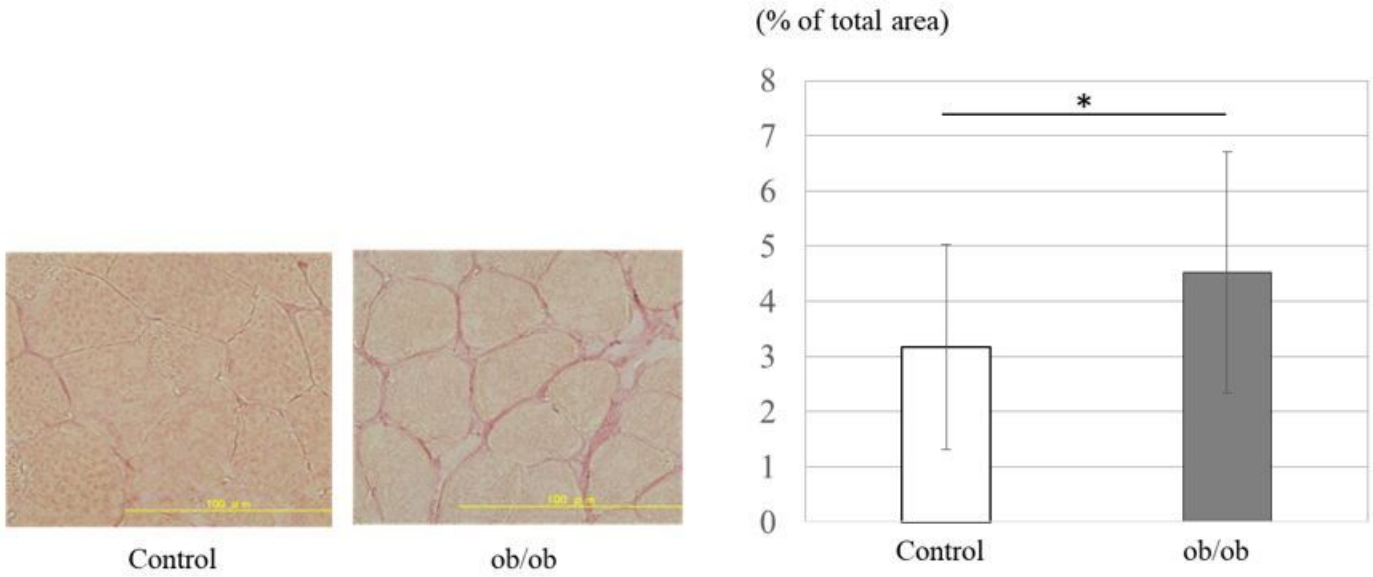

Figure 4

Collagen deposition The areas of collagen deposition are significantly larger in ob/ob mice compared with the controls. * p<0.05.

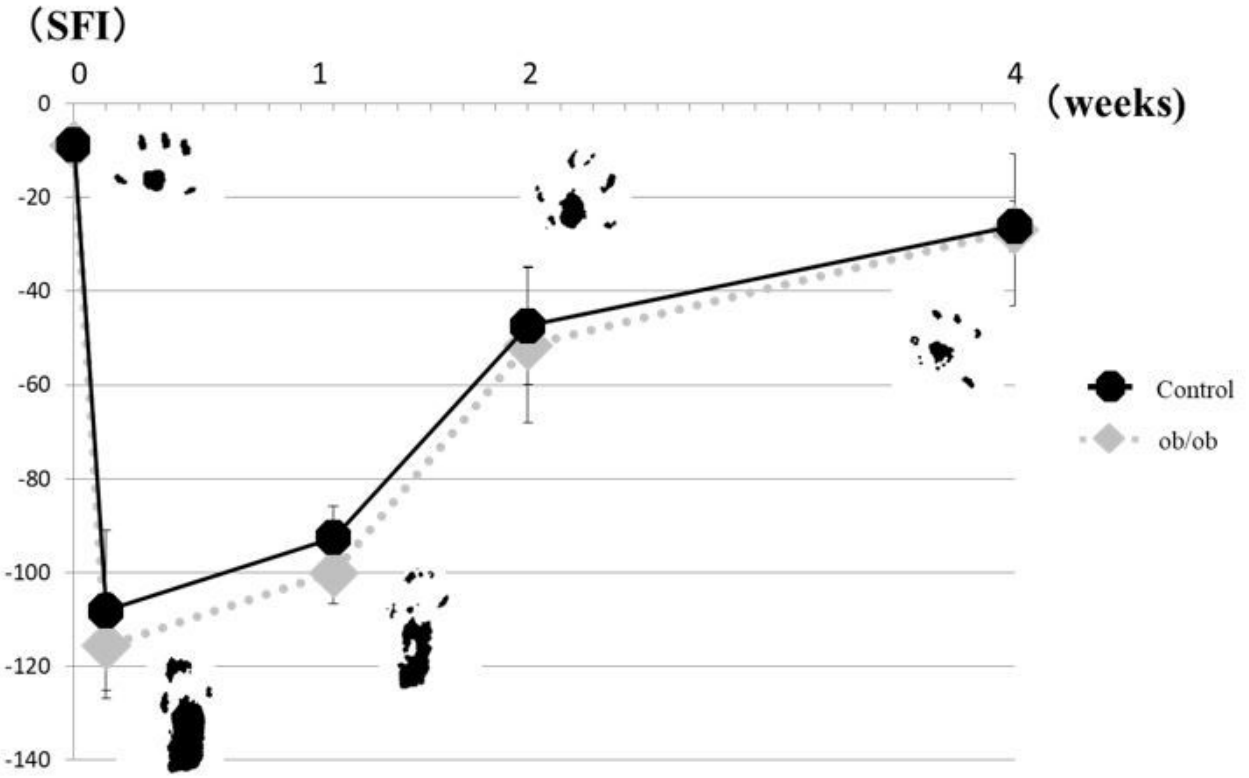

Figure 5

Sciatic functional index SFI was immediately reduced after crush and then gradually improved. A significant difference was not observed between the two groups.

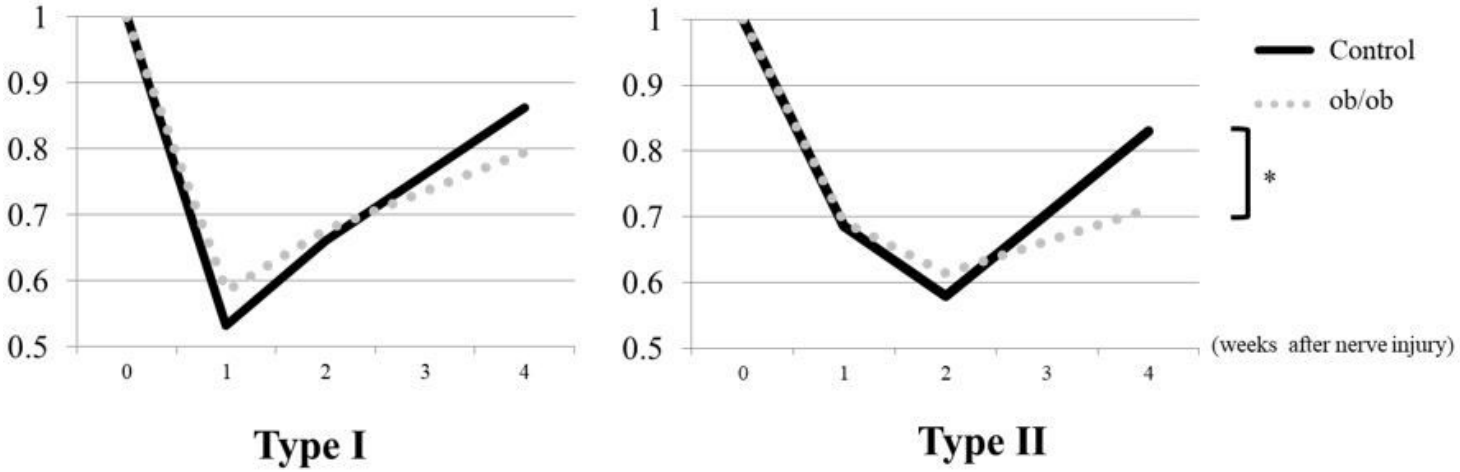

Figure 6

Cross-sectional area of gastrocnemius after sciatic nerve crush The cross-sectional area of the muscle fiber decreased after nerve crush, and then improved. The cross-sectional area of the type II muscle fiber is significantly poorly improved in the ob/ob mice. There is no obvious difference in type I. * p<0.05

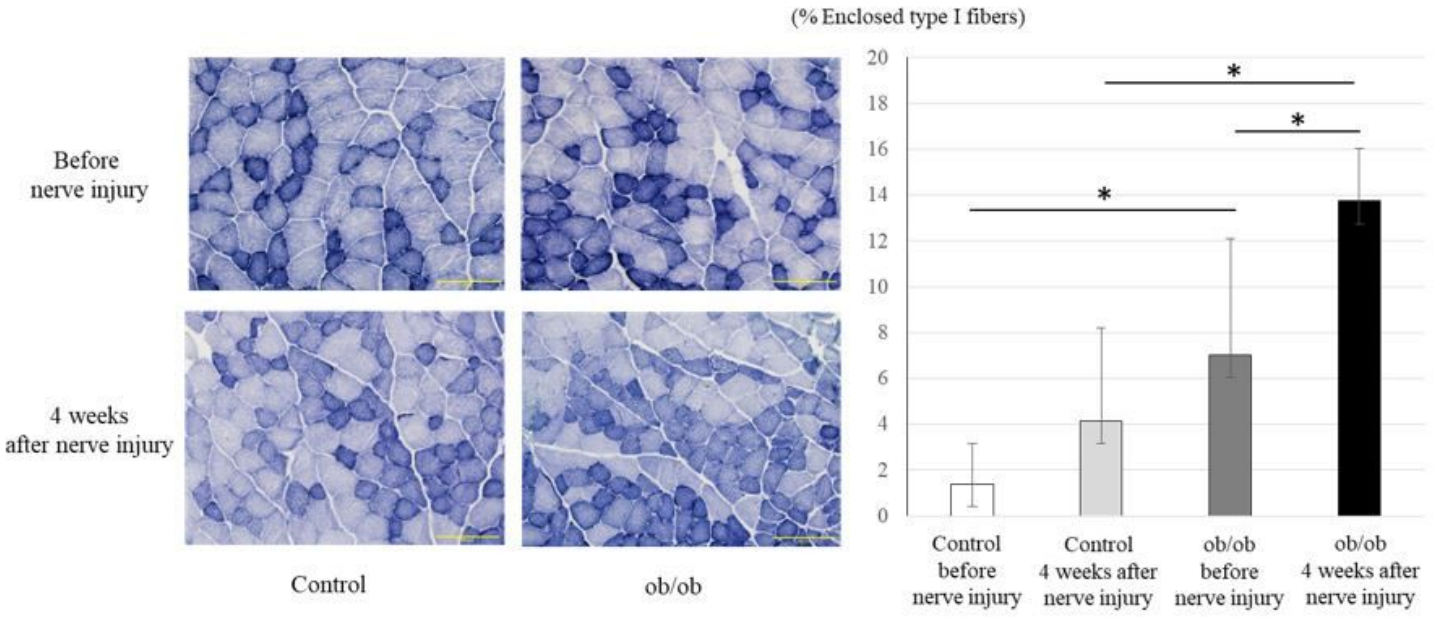

Figure 7

Enclosed Type I fibers Enclosed Type I is significantly increased after nerve crush. This is especially noticeable in the ob/ob mice. * p<0.05.

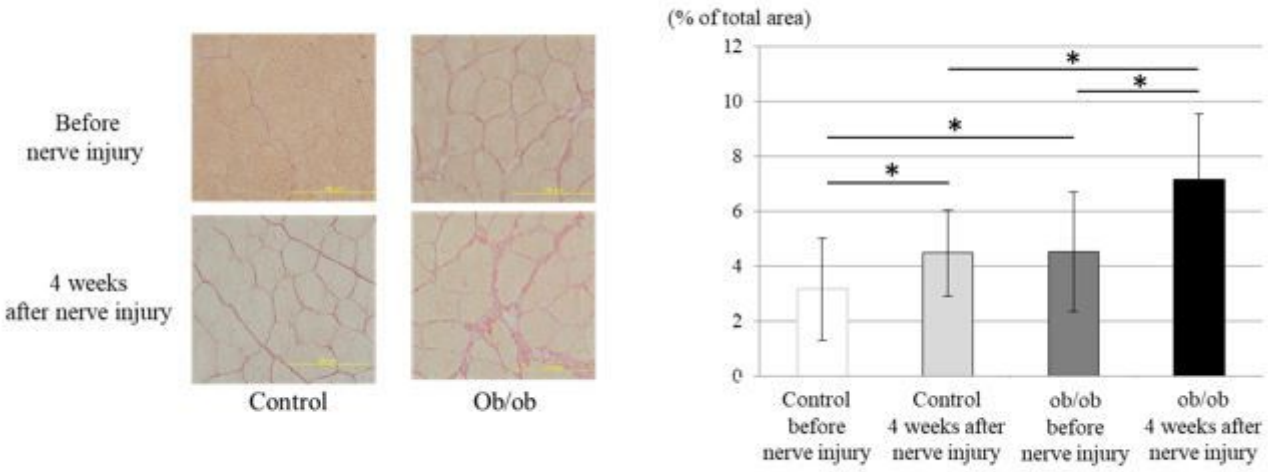

Figure 8

Collagen deposition after nerve crush The cross-sectional areas of collagen deposition at intermyofibers are significantly larger than before the nerve crush. In ob/ob mice, the increase of collagen deposition after the nerve injury was significantly higher compared to the control. * p<0.05.

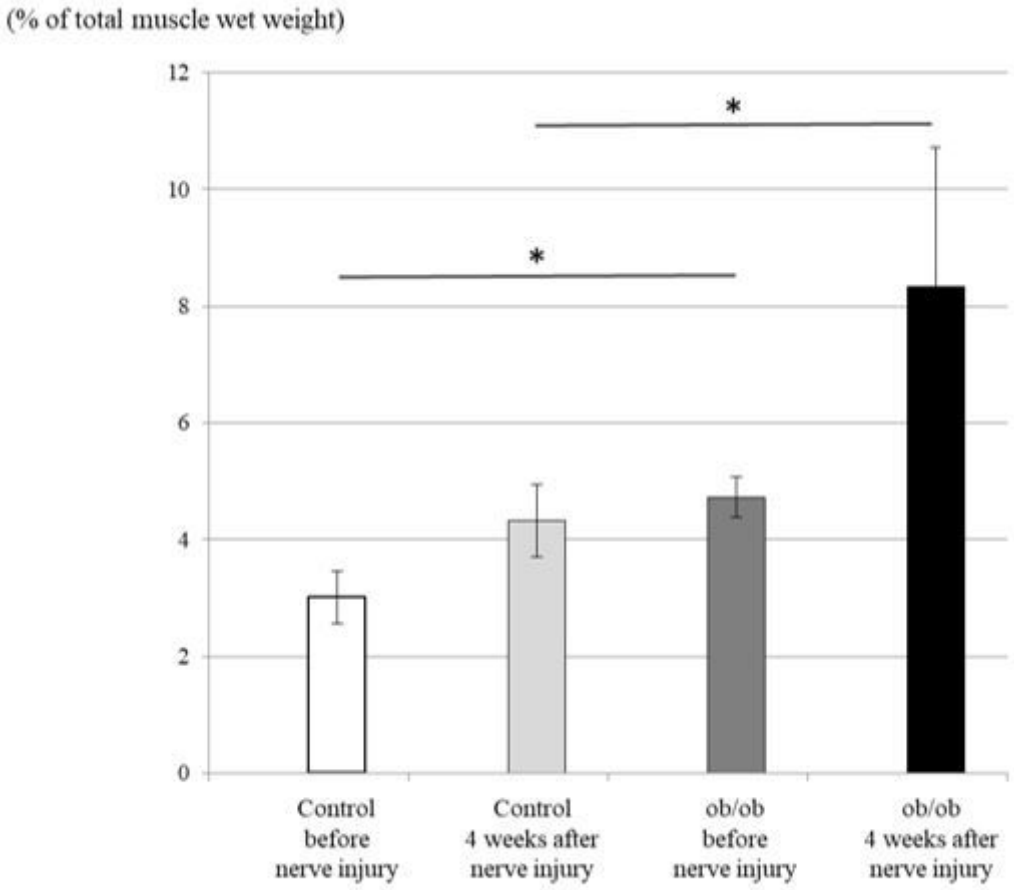

Figure 9

Collagen assay The collagen content in skeletal muscle is increased after nerve crush in both groups. In ob/ob mice, the amount of collagen is markedly increased compared to the control group. * p<0.05.